



Evaluating the combined effect of photooxidation and thermal ageing of bitumen

Johannes Mirwald, Bernard Maric, Kristina Primerano & Bernhard Hofko

To cite this article: Johannes Mirwald, Bernard Maric, Kristina Primerano & Bernhard Hofko (30 Jan 2025): Evaluating the combined effect of photooxidation and thermal ageing of bitumen, Road Materials and Pavement Design, DOI: [10.1080/14680629.2025.2456919](https://doi.org/10.1080/14680629.2025.2456919)

To link to this article: <https://doi.org/10.1080/14680629.2025.2456919>



© 2025 The Author(s). Published by Informa UK Limited, trading as Taylor & Francis Group.



Published online: 30 Jan 2025.



Submit your article to this journal [↗](#)



Article views: 301



View related articles [↗](#)



View Crossmark data [↗](#)

Evaluating the combined effect of photooxidation and thermal ageing of bitumen

Johannes Mirwald , Bernard Maric, Kristina Primerano  and Bernhard Hofko 

Christian Doppler Laboratory for Chemo-Mechanical Analysis of Bituminous Materials, Institute of Transportation, TU Wien, Austria

ABSTRACT

Up to date, mainly temperature or UV light is incorporated into laboratory bitumen ageing procedures. However, the impact of visible light showed some interesting results recently. Therefore, an unmodified binder was exposed to a combination of temperature and different sun and narrow UV and blue light lamps. The aged binders were analysed with Fourier Transform Infrared (FTIR) spectroscopy, dynamic shear rheometer (DSR) and SARA fractionation. The results showed synergistic effects between temperature and light. Surprisingly, different lamp intensities lead to almost the same level of ageing, indicating that merely a certain amount of photoenergy is needed. Lastly, comparing the UV and blue light domain to sunlight showed that while exposed to the same amount of photoenergy, its effect on rheology differs, where sunlight showed the most impact on ageing. This highlights the importance of sunlight to the ageing process to sufficiently understand its combination with other ageing inducing factors.

ARTICLE HISTORY

Received 13 March 2024
Accepted 10 January 2025

KEYWORDS

Bitumen; photooxidation; FTIR spectroscopy; DSR; chemo-mechanics; SARA fractionation

1. Introduction

The investigation of the bitumen ageing mechanism has been in the focus of research for more than 40 years (Petersen, 1984). Due to the material's molecular complexity and diversity caused by different crude oil origins, a simplified oxidation mechanism and model is not easily accessible. This becomes even more complex when different environmental ageing inducing factors such as temperature, light, rain, moisture or reactive oxygen species from the troposphere need to be considered in their individual or combined effects. The impact of temperature has been well documented in the past and present (Adolfo et al., 2022; Camargo et al., 2020; Petersen, 2009; Petersen & Glaser, 2011). This led to the current standardised binder long-term ageing procedure in the laboratory: the pressure ageing vessel (PAV) test, which only includes temperature at 90–100°C and an increased pressure of 2.1 MPa as ageing inducing factors. While this can bring the binder into a heavily oxidised state, its correlation to real field ageing is questioned, since many other environmental factors are neglected (Mirwald et al., 2020; Petersen, 2006). This led to the development of different laboratory long-term ageing setups and devices that try to incorporate other environmental ageing inducing factors. A factor not often considered in bitumen ageing experiments is the gas atmosphere. The majority of laboratory experiments use normal, compressed air. However, reactive oxygen species (ROS), like ozone (O₃), nitrogen oxides (NO_x) or hydroxyl radicals (OH), can play a crucial role in the oxidation process occurring in the field. Some of these ROS like ozone or hydroxyl radicals are naturally occurring in the troposphere at a low concentration. Other species like nitrogen oxides are produced by diesel car's engines (Atkinson, 2000) and can affect binder ageing significantly. This was demonstrated by studies on the binder

CONTACT Johannes Mirwald  johannes.mirwald@tuwien.ac.at

© 2025 The Author(s). Published by Informa UK Limited, trading as Taylor & Francis Group.

This is an Open Access article distributed under the terms of the Creative Commons Attribution License (<http://creativecommons.org/licenses/by/4.0/>), which permits unrestricted use, distribution, and reproduction in any medium, provided the original work is properly cited. The terms on which this article has been published allow the posting of the Accepted Manuscript in a repository by the author(s) or with their consent.

(Hofer et al., 2022; Mirwald et al., 2020), loose mix (Sreeram et al., 2021) and compacted asphalt mixture level (Maschauer et al., 2020). Even the presence of individual ROS species, such as NO_x , can accelerate binder oxidation significantly (Hofer et al., 2022), thus showing the importance of the ageing atmosphere.

Beside the ageing atmosphere, other environmental factors like moisture or water can contribute to binder ageing via moisture induced damage. Various theories of the involved mechanisms on the molecular level have been reported by Ma et al. (2021), concluding that mostly diffusion, sorption and clustering need to be considered for ageing. Furthermore, work by Hung et al. (2017) showed that polar components are allocated near the surface after exposure to water, which demonstrates that various interactions between water and bitumen can occur and need to be considered, especially at elevated temperatures. Beside the active role of water in the ageing process, another, passive contribution via the formation of OH radicals in the tropospheric cycle can also contribute to oxidation of organic matter. Water in combination with ozone and light can produce these radicals, which feed the tropospheric cycle. However, the quantification of such OH radicals and their precise mechanism is mostly unexplored in connection with bitumen ageing.

The last and second most used ageing inducing factor besides increased temperature in the incorporation of light. Looking at the literature, whenever researchers around the world have implemented light into a binder ageing setup it was mostly focused on the UV domain (Feng et al., 2015; Hung et al., 2019; Hung & Fini, 2020; Li et al., 2019; Zeng et al., 2018). Many of these studies used narrow band UV light lamps or sun light lamps that focus on the UV-A and UV-B domain between 290–390 nm (de Sá Araujo et al., 2013; Hofer et al., 2022; Hu et al., 2022; Zeng et al., 2018). In theory, this approach seems reasonable since light of a low wavelength exhibits a high level of photoenergy. However, Mirwald et al. (2022a) found evidence that also visible light can contribute significantly to the bitumen ageing process, especially when considering the absorption effect of earth's atmosphere. These atmospheric absorption effects by the ozone layer strongly reduce the amount of UV light reaching earth's surface, while visible light is mostly passing through. Thus, visible light can be found at a much higher intensity on the pavement surface. This effect was investigated by using 15 different wavelength domains ranging from 365 to 770 nm. The respective lamp intensities were adjusted to mimic conditions on earth's atmosphere. These purely photo-oxidised binders were investigated with ATR-FTIR spectroscopy, which revealed that blue light is able to oxidise the material more than the higher energetic UV light, when considering the conditions on earth's atmosphere. The drawback of this study is that these effects were purely caused by photooxidation. No combination with other ageing inducing factor, such as temperature, was investigated. Furthermore, no correlation to its effect on rheology was measured, since the samples were investigated from a purely surface related analysis perspective. This raises the question how visible light compares to UV light and interacts with other ageing inducing factors like elevated temperature.

Thus, this study intends to investigate the effect of combining elevated temperatures and different visible and UV light domains as well as different light intensities on an unmodified short-term aged binder. Comparison to its individual ageing inducing factors, pure temperature or light induced ageing will be made to reveal the synergistic effect of these two parameters. The binders will be analysed with FTIR spectroscopy, dynamic shear rheometer (DSR) and polarity-based separation into the four SARA fractions (Saturates, Aromatics, Resins and Asphaltenes). Correlations between chemical and rheological information will be made by the so-called chemo-mechanical correlation, linking the formation of oxidised functional groups with the increase in stiffness.

2. Materials and methods

2.1. Materials and sample preparation

In this study, a non-modified 70/100 penetration graded binder was used. The basic properties of the binder are as follows:

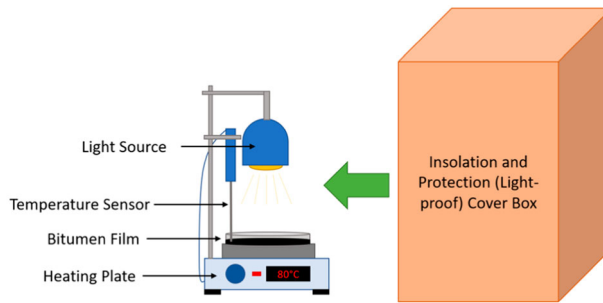


Figure 1. Schematic drawing of the ageing setup.

Table 1. Details for the lamps used in this study.

Lamp	Wavelength [nm]	Intensity at 20 cm distance [W/m^2]
Reptile Bright Sun UV Desert	290 – 800	2.25
Thorlabs Solis 3C	400–750	660
Thorlabs Solis 365C	365	660
Thorlabs Solis 405C	405	660

- Penetration grade (1/10 mm): 84
- Softening point ($^{\circ}C$): 45.8
- Performance grade: 58–28.

Since various long-term ageing experiments were conducted in this study, a short-term ageing (STA) state had to be reached prior to the ageing experiments. Thus, for the light ageing experiments 8 g of the unaged 70/100 penetration graded binder were heated to $140^{\circ}C$, homogenised and poured in a metal PAV container. To ensure that the binder forms an even film and reaches short-term ageing level simultaneously, it was stored in the oven at $163^{\circ}C$ for 75 min. This STA binder was then placed into the ageing setup described in Section 2.2 which is schematically shown in Figure 1.

Additionally, to compare the results obtained from the light ageing experiments multiple laboratory ageing cycles using the pressure ageing vessel (PAV) method were conducted following the EN 14769 (CEN, 2012a). Therefore, short-term aged binder (following the En 12607-1 (CEN, 2015)) was poured into the respective metal containers and aged at $100^{\circ}C$ and 2.1 MPa for 20 (1x), 60 (3x) and 80 (3x) hours of ageing.

2.2. Light ageing setup and ageing program

The light ageing setup consists of a standard laboratory heating plate (with a temperature sensor attached to the heating plate), a light source and an isolation and protection cover box, shown schematically in Figure 1. The lamps were fixed at a distance of 20 cm, which was correlated to the calibration process of the lamps.

During the study four different lamps were used, with their respective details shown in Table 1. The two sun light lamps (Reptile Bright Sun UV Desert and Thorlabs Solis 3C) exhibited different intensities (ratio of 1:300). All three Thorlabs lamps were used at the same intensity ($660 W/m^2$). This intends to provide information how significant the influence of the lamps powers is and whether the impact of the respective wavelength domain can be compared to recent work on visible light ageing (Mirwald et al., 2022a).

For a light ageing experiment (with light and elevated temperature), the metal container with the 8 g of STA binder was placed on the heating plate (set to $90^{\circ}C$) for a duration of 3 days and the respective lamp was switched on. The temperature sensor attached to the heating plate was dipped into the

binder film, to ensure that the binder would maintain a constant temperature of 80°C. This allowed constant temperature control over the course of the entire ageing duration. For the pure light ageing experiments (without the addition of the heating plate), the temperature sensor was also used to track whether the lamps themselves induce an increase in temperature of the binder films (which was not observed). After the 3 days of ageing, the binder was placed in a preheated oven at 150°C to melt and homogenise the aged material and collect it. Two to three repetitions per ageing condition were conducted and evaluated.

2.3. Methods

2.3.1. Attenuated total reflection Fourier-transform infrared (ATR-FTIR) spectroscopy

For ATR-FTIR spectroscopy, a Bruker Alpha II was used. The spectrometer is equipped with an ATR unit containing a diamond crystal and a deuterated triglycine sulphate (DTGS) detector. For each ageing state, a small quantity of the respective binder was heated to 140°C for a maximum of 1 min, taking recent literature suggestions into account (Mirwald et al., 2022b). Once the binder reached a liquid state, four small binder droplets were poured onto suitable substrates (silicone paper) after ensuring proper homogenisation using a thermometer. Once the samples have cooled down (~5 min), the spectra were recorded within a spectra range of 4000–680 cm⁻¹ at a resolution of 4 cm⁻¹ and 24 scans. Each sample was measured with four repeats, resulting in a total of 16 spectra per binder (as four different droplets were measured). For spectral evaluation, a min–max normalisation between 3200 and 2800 cm⁻¹ was used, followed by a full base line integration using the following limits:

- Carbonyls (Al_{CO}): 1660–1800 cm⁻¹
- Sulfoxides (Al_{SO}): 1079–984 cm⁻¹
- Reference aliphatic band (Al_{CH_3}): 1525–1350 cm⁻¹.

The Ageing Index (AI) according to Equation (1) provides information on the uptake in oxygen due to the different ageing process caused by temperature and light ageing.

$$AI_{FTIR} = \frac{(Al_{CO} + Al_{SO})}{Al_{CH_3}} \quad (1)$$

The respective contributions of each of the functional groups is shown by an indicator in the respective figures (see Figure 3 and Figure 9). These ageing indices represents the mean value and standard deviation from the 16 spectra recorded by binder and will be shown in addition to a selected choice of individual spectra per binder in the results in Figure 2, Figure 6 and Figure 9.

2.3.1.1. Dynamic shear rheometer (DSR). To assess the rheological behaviour of the material, a dynamic shear rheometer MCR 302 from Anton Paar was used. For sample preparation, the binders were shortly heated and homogenised to a maximum of 140°C and filled into a 25-mm silicon mould. The sample in the mould was stored for 24 h in the dark before being measured following the EN 14770 (CEN, 2012b). The following frequencies and temperatures were used in the experiments:

0.1, 0.3, 1, 1.592, 3, 5, 8 and 10 Hz

40, 46, 52, 58, 64, 76 and 82°C

The results display the respective G^* and phase angle values at 1.59 Hz across the measured temperature domain and are shown in the results in Figure 4, Figure 7 and Figure 10.

Table 2. Overview of the solvents and their respective ratios used for separation.

Fraction	Quantity [ml]	Solvent	Ratio [vol%]
Prewash	20	<i>n</i> -Heptane	100
Saturates	10	<i>n</i> -Heptane	100
Aromatics	25	Toluene: <i>n</i> -Heptane	80:20
Resins	40	Dichloromethane: Methanol	90:10

2.4. Chemo-mechanical correlation

The chemo-mechanical correlation links the uptake from oxygen via the formation of functional groups from FTIR spectroscopy in the micrometre domain to rheological properties of the material from the DSR in the millimetre domain. This is done by plotting the norm of the complex modulus $|G^*|$ at 1.592 Hz and 46°C versus the FTIR ageing index including carbonyls and sulfoxides. This visualises how changes in stiffness can be linked to the incorporation of oxygen via the formation of functional groups.

2.5. SARA fractionation

To separate the binders into the four polarity-based SARA fractions, a novel solid phase extraction (SPE) method developed by Razouki and Ibrahim (2018) was used. In this separation, 400 ± 20 mg of the binder are dissolved in 40 ml of *n*-heptane and stirred at room temperature for 24 ± 2 h. The asphaltenes are then separated using a syringe and a filter (Thermo Scientific™ Titan3™ PTFE syringe filters with a diameter of 25 mm and a pore size of 0.2 μm). The maltene solution (15 ml) was diluted to 3.33 mg/ml and applied onto an SPE cartridge (Thermo Scientific™ HyperSep™ Silica SPE cartridges with a pore size of 40–63 μm) that was mounted on a vacuum manifold. After prewashing of the cartridge and application of the maltene solution, the three remaining fractions were eluted using the solvents listed in Table 2.

After the separation process, the solvent was evaporated using a heating plate and a continuous nitrogen stream (to avoid additional oxidation). A portion of the maltenes as well as the separated SAR fraction solutions were then evaporated under a nitrogen atmosphere and weighed to determine the gravimetric distribution of the maltenes and respective separated fractions the binders.

3. Results

The results will be split into three sections. First off, the two different sun light lamps with different photoenergies will be compared, followed by their comparison to standardised laboratory ageing (1x PAV, 3x PAV and 4x PAV). Finally, one of the sunlight lamps (from Thorlabs) will be compared to specific wavelength domains (also Thorlabs at 365 and 405 nm), which will provide insight how a full range spectrum compares to previous literature, where specific wavelength regions were investigated (Mirwald et al., 2022a). The results are structured to discuss the spectroscopic results first, showing the respective spectra and resulting indices (see Figure 2, Figure 3, Figure 6 and Figure 9), followed by the rheological results from the DSR (see Figure 4, Figure 7 and Figure 10). Furthermore, the chemo-mechanical correlation from FTIR spectroscopy and DSR will be shown and discussed for each of the three sections (see Figure 5, Figure 8 and Figure 11). The influence of pure photoaged binders will always be displayed in a bright colour (green, blue or purple), while their respective combination with temperature will be shown in the same, darker colour (also green, blue or purple). Finally, the results of SARA fractionation from the binders aged by the three different Thorlabs lamps (sunlight – 3C, 365 and 405 nm) will be shown and discussed (Figure 12).

3.1. Comparison of different sun light lamps

Figure 2 shows the FTIR spectra and the fingerprint region of the two different sun light lamp aged binders at elevated temperatures of 80°C (dark green and blue) and at room temperature (bright green and blue) as well as the pure thermal reference aged binder (aged at 80°C – orange) and initial starting STA binder (red).

The impact of pure photooxidation of both lamps is very limited, as there is no significant difference in the red, bright green and bright blue spectra, which are almost overlapping. This is confirmed by the evaluation of the ageing indices shown in Figure 3. This can be explained by the fact that light is only able to penetrate up to a maximum of its wavelength into the material. Since the binder film has a thickness of ~ 0.5 mm (500,000 nm) the light of around 500 nm will only affect 0.1% of the material. It should also be kept in mind that the binders were completely homogenised after each ageing experiment, to provide the same conditions as for other laboratory ageing procedures (PAV) or the recovery process from the field, where the binder is also homogenised during recovery.

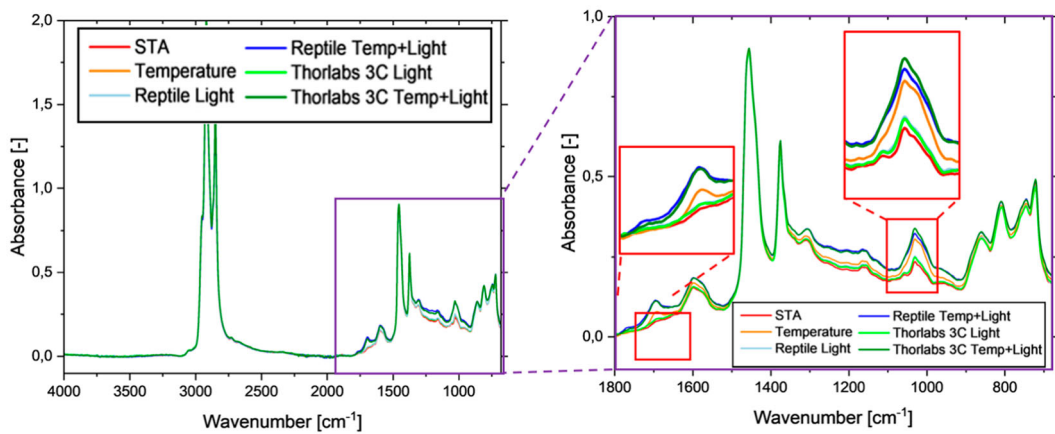


Figure 2. FTIR spectra (left) and fingerprint region between 1800 and 680 cm^{-1} (right) of the STA (Red), pure temperature aged (orange) and binders aged with Thorlabs 3C lamp (green) and Reptile Sun UV (blue).

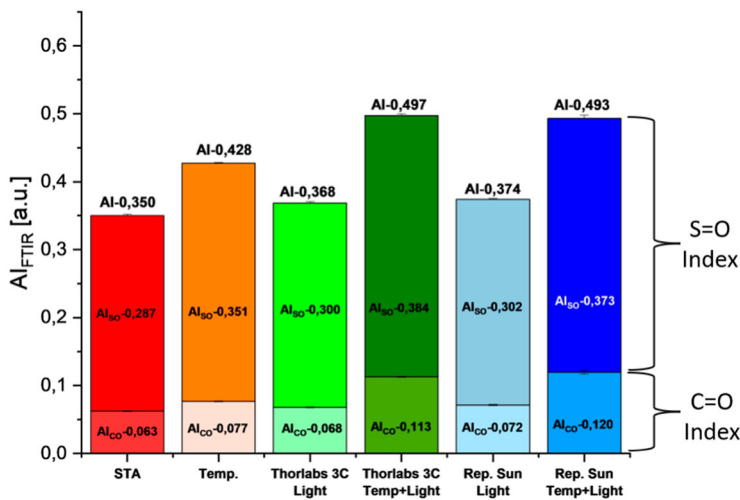


Figure 3. FTIR ageing indices of the STA (Red), pure temperature aged (orange) and binders aged with Thorlabs 3C lamp (green) and Reptile Sun UV (blue).

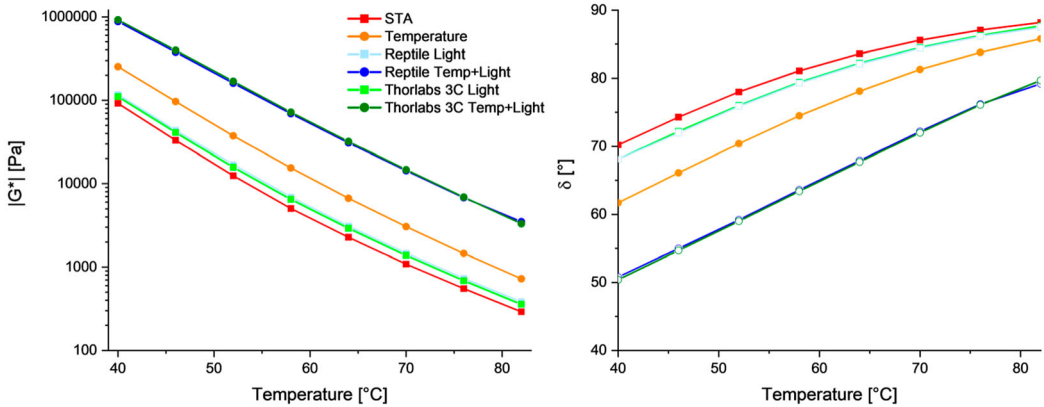


Figure 4. Norm of the complex modulus $|G^*|$ at 1.59 Hz (left) and phase angle (right) of the STA (Red), pure temperature aged (orange) and binders aged with Thorlabs 3C lamp (green) and Reptile Sun UV (blue).

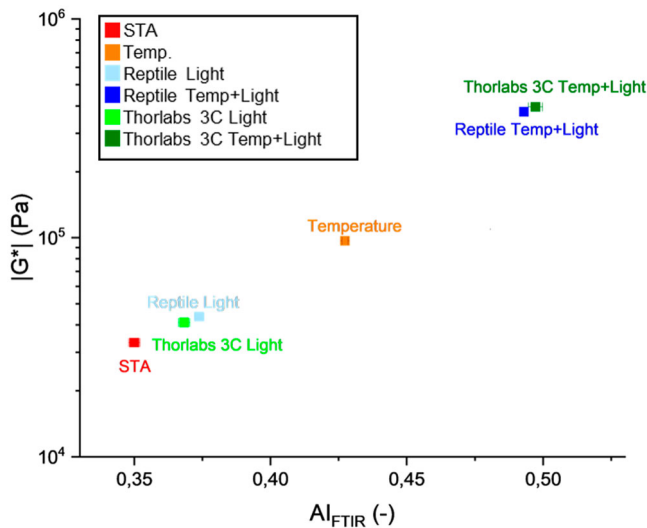


Figure 5. Chemo-mechanical correlation of the of the STA (Red), pure temperature aged (orange) and binders aged with Thorlabs 3C lamp (green) and Reptile Sun UV (blue).

The influence of temperature (orange) is noticeable, where both ageing related functional groups, carbonyls and especially the sulfoxides are forming (Petersen, 2009). Combining the sun light lamps with temperature (blue and green spectra), a significant increase in the carbonyl region is observable, while the sulfoxide band is only increasing insignificantly, compared to pure thermal ageing (orange). This indicates that most of the sulfoxide formation is temperature driven, while the addition of the photoenergy leads to the additional formation of carbonyls. Furthermore, a shoulder around 1750 cm^{-1} can be seen, which corresponds to an OH band that can be assigned to alcohols, esters, carboxylic acids or anhydrides (Larkin, 2011; Petersen et al., 2002). However, a precise assignment to one of these functional groups is not yet possible without further analysis using NMR spectroscopy or other molecular analysis methods.

Figure 3 shows the FTIR aging indices from the different sun light lamps (in blue and green) as well as the pure thermal reference ageing (orange) and initial short-term aged samples (red). These

indices quantify the observations and assumptions from the previous spectra and confirm the previously mentioned trends. The influence of pure light shows no significant formation of carbonyls and sulfoxides compared to the initial STA state. The temperature induced ageing (orange) is mainly producing sulfoxides, while the combined factors lead to the overall highest ageing levels, producing both carbonyls and sulfoxides. Interestingly, even though both lamps exhibit different light energy levels, as highlighted in Table 1, no significant differences in the resulting ageing products detectable with FTIR spectroscopy can be observed. This can provide first evidence that the amount of photoenergy is not the oxidation limiting resource in the ageing process and that only a certain amount of photoenergy is needed. However, further experiments are needed to confirm this assumption.

Figure 4 shows the results of the rheological investigation with the norm of the complex modulus $|G^*|$ at 1.59 Hz displayed on the left side and the phase angle on the right side. Similar to the trends in FTIR spectroscopy, the impact of visible light without the combination to temperature (bright green and bright blue) does not lead to significant changes in the rheological properties of the binder. The influence temperature alone (orange) leads to a noticeable increase in stiffness and decrease in the phase angle. However, the combination of both ageing inducing factors shows the synergistic effect, resulting in a significant increase in the complex modulus and decrease in the phase angle. Similar to FTIR spectroscopy, both lamps, despite differences in their intensities, lead to a similar rheological level.

The chemo-mechanical correlation in Figure 5 shows how changes in the chemical composition by the formation of oxygen containing functional groups like carbonyls and sulfoxides can be linked to changes on the rheological level by an increase in stiffness. Starting at the initial STA sample (red), which is allocated close to the axis origin, showing the lowest level of aging. After pure light ageing (bright green and blue), merely the previously mentioned small increase in ageing is clearly observable. Pure temperature induces ageing is significantly above this. However, by far the highest ageing level can be seen when both ageing inducing factors are combined. This highlights the synergistic effect between light and temperature, as adding both individual values from light and temperature would not lead to the same increase in ageing levels. Furthermore, an interesting observation is made when comparing the ageing level of both sun light lamps, which have a large discrepancy between their respective power (factor of 1: ~ 300). These ageing levels are very close to each other, which indicates that only a certain amount of photo energy is needed to induce this synergistic effect of photo-temperature induced ageing. Thus any excess photoenergy will not lead to additional ageing.

3.2. Comparison of sun light and standardised laboratory ageing

Figure 6 compares the FITR spectra from the previous sun light ageing series to standardised laboratory aged samples using the PAV. The left side of Figure 6 shows how the 1x PAV (20 h – yellow), 3x (60 h – turquoise) and 4x PAV (80 h – purple) aged binders compare against the pure temperature induced ageing (72 h – orange). Here, it can be seen how significant the influence of the high pressure for the PAV is, as the 72 h of pure temperature ageing led only to a slightly higher ageing level than 20 h of PAV ageing. However, the ageing level is significantly lower than that of the 60 and 80 h PAV aged binders. The right side of Figure 6 compares both sun light lamp aged binders, which are allocated between the 3x PAV and 4x PAV.

Figure 7 shows the comparison of the rheology results from the sun light ageing series and the PAV ageing series. Similar to results from FTIR spectroscopy, the order regarding pure temperature aged binder (orange) and the PAV ageing series remains the same. Surprisingly, the stiffness and phase angle of both sun light and temperature aged binders (dark green and blue) show a significantly higher ageing level than the 4x PAV aged binders. Thus, the trends do not align with FTIR spectroscopy, which indicated that not all rheological changes are captured by the two functional groups in infrared spectroscopy.

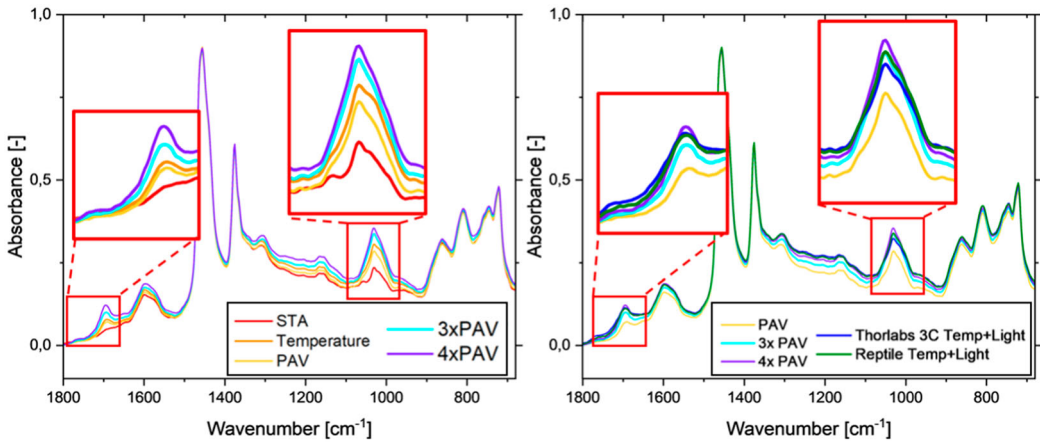


Figure 6. Comparing FTIR spectra of the sun light ageing series and 1x PAV (yellow), 3x PAV (turquoise) and 4x PAV (purple).

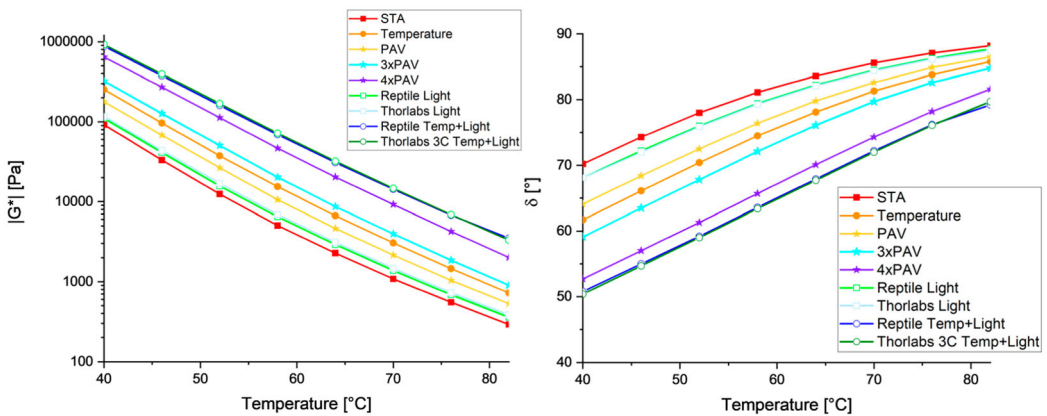


Figure 7. Norm of the complex modulus $|G^*|$ at 1.59 Hz (left) and phase angle (right) of the STA (Red), pure temperature aged (orange) sun light lamp aged with Thorlabs 3C lamp (green) and Reptile Sun UV (blue) as well as 1x PAV (yellow), 3x PAV (turquoise) and 4x PAV (purple).

Figure 8 summarised both previously shown PAV methods in the chemo-mechanical correlation where the results from the sun light lamps study are compared against the PAV aged binders. The most interesting observation is that the light aged binders (dark green and blue) exhibit a similar level in infrared spectroscopy, but show higher rheological values, indicating that FTIR spectroscopy (or its evaluation method) might not be capable to entirely capture the chemical changes caused by light and temperature induced ageing that result in such mechanical changes. This will require a deeper investigation on the molecular level from an alternative perspective to detect possible differences in the respective ageing mechanism.

3.3. Comparison of different wavelength domains

In the last section of the results (Figure 9), the FTIR spectra and ageing indices of the three different Thorlabs lamps (365 nm, 405 nm and sunlight lamp) are shown. It needs to be kept in mind that all lamps were used at the same intensity level (660 W/m^2), as shown in Table 1. The results indicate that all three lamps induce no significant ageing without an increase in temperature. Similar to the sun light lamps, most of the sulfoxides are formed during thermal ageing, while all three lamps induce

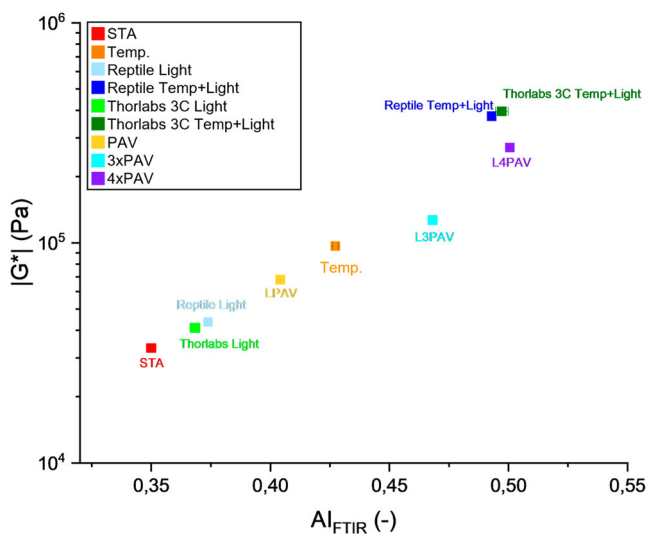


Figure 8. Chemo-mechanical correlation of the STA (Red), pure temperature aged (orange) sun light lamp aged with Thorlabs 3C lamp (green) and Reptile Sun UV (blue) as well as 1x PAV (yellow), 3x PAV (turquoise) and 4x PAV (purple).

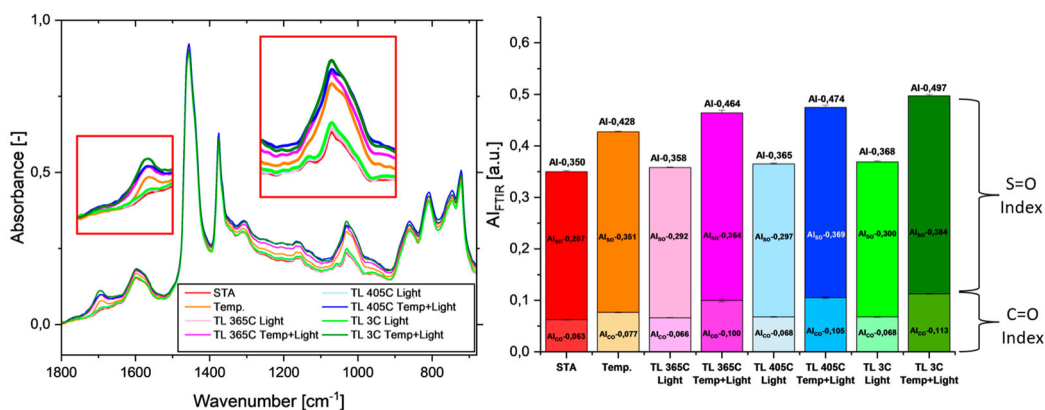


Figure 9. FTIR spectra (left) and FTIR ageing indices (right) of the reference STA binder (Red), pure temperature aged binder (orange) and binders aged with Thorlabs 365 nm lamp (purple), Thorlabs 405 nm lamp (blue) and Thorlabs SOLIC 3C lamp (green).

an increase in the carbonyl and the alcohol/ester/acid/anhydride region (1750cm^{-1}) (Larkin, 2011; Petersen et al., 2002). Minor differences in the shape of the sulfoxide band are observed for the 405 nm aged binder (blue), where a distinctive shoulder can be seen just below the usual band at 1030cm^{-1} . However, no clear functional group assignment can be made yet. Comparing the three different sun light lamps, it can be said that the highest ageing level was achieved with the sun light lamp, followed by the 365 and 405 nm lamps. This indicates that a combination of different wavelength domains is more effective when considering the impact of solar irradiation.

Figure 10 displays the results from rheology, where an interesting trend can be observed when comparing the impact of the different wavelength domains in the complex modulus (left) as well as the phase angle (right).

While the usual trends with individual contributions of pure light (bright purple, blue and green) and temperature (orange) are insignificant or well predictable, the influence of the different wavelength domains in combination with elevated temperatures show an unpredicted result. A significant

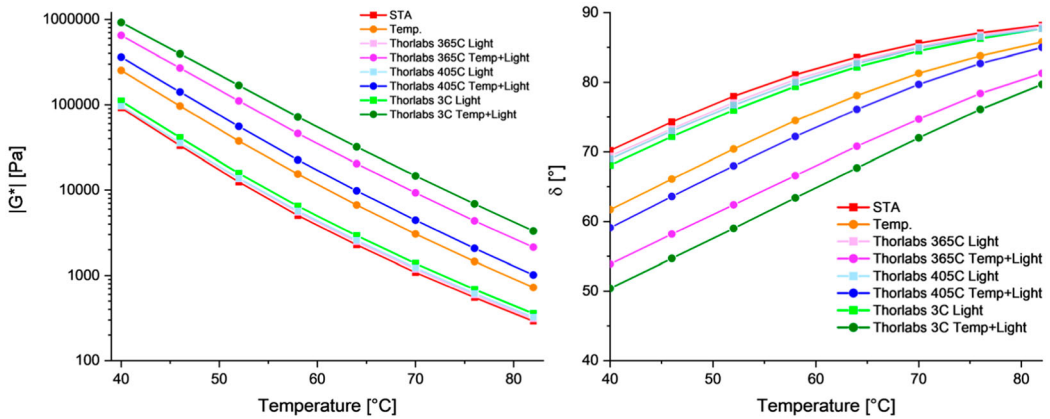


Figure 10. Norm of the complex modulus $|G^*|$ at 1.59 Hz (left) and phase angle (right) of the reference STA binder (Red), pure temperature aged binder (orange) and binders aged with Thorlabs 365 nm lamp (purple), Thorlabs 405 lamp (blue) and Thorlabs SOLIC 3C lamp (green).

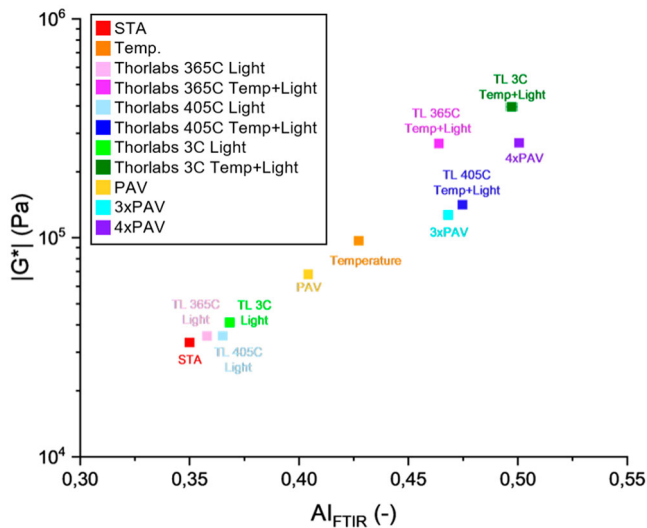


Figure 11. Chemo-mechanical correlation (right) of the reference STA binder (Red), pure temperature aged binder (orange) and binders aged with Thorlabs 365 nm lamp (purple), Thorlabs 405 lamp (blue) and Thorlabs SOLIC 3C lamp (green).

difference between blue (405C), UV (365C) and sun light (3C) are observable in terms of stiffness levels, with the blue light showing less impact on the rheological properties compared to the UV and sun light lamp.

This difference becomes well pronounced when correlating results from FTIR spectroscopy to rheology in the chemo-mechanical correlation (see Figure 11). Here the difference in the ageing levels from the three wavelength domains become obvious, as the 405 nm aged binder (blue) is very close to the ageing level of the 3x PAV aged binder. The 365 nm aged binder has a similar formation of carbonyls and sulfoxides as the 3x PAV aged binder, but its rheological level is close to the 4x PAV aged binder. Lastly, the sun light aged binder shows the highest ageing level, surpassing the 4x PAV aged binder on the rheological domain, while being close in terms of carbonyl and sulfoxide content. To understand these unpredictable results in the chemo-mechanical correlation, it might be useful to

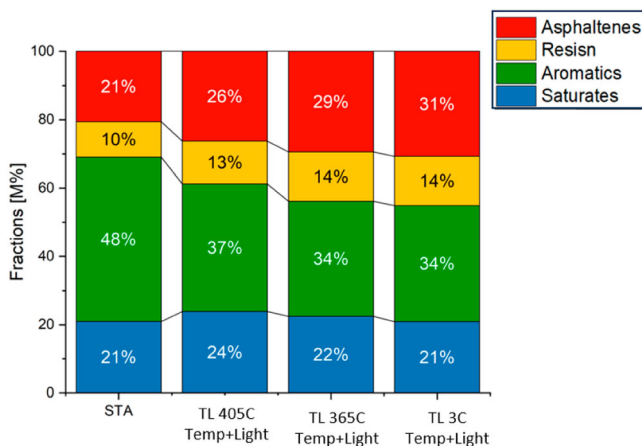


Figure 12. SARA fractions of the STA, and all three Thorlabs aged binders.

consider a different perspective to judge the binders ageing level, since FTIR spectroscopy only captures IR active functional groups. Furthermore, it might be that the evaluation of the ageing indices is not ideal for these samples (different integration methods, etc.) or that these methods simply do not correlate perfectly with each other when investigating the impact of photooxidation of different wavelength domains, as respective changes might not be captured.

Thus, another factor for assessing ageing from a different perspective was investigated: the impact of the different wavelengths on the distribution of the SARA fractions. The respective results of the three different Thorlabs lamps as well as the initial STA binder are shown in Figure 12. These results show a similar trend as seen in rheology with the 405 nm lamp inducing a lower change in the polarity gradient, followed by the 365 nm and sun light lamps. It should be noted that the intensities of all three Thorlabs lamps were adjusted to the same level of power. Therefore, a comparison to conditions on earth's surface is not yet given. Nonetheless, it becomes obvious that the respective light induced on the sample surface seems to play a crucial role in regard to the ageing levels induced. However, further testing in regard to adjusted light intensities and establishing a link between the polarity gradient, functional group content and the rheological behaviour are necessary in the future.

Conclusion

This study investigated the impact of photooxidation with and without its combination to thermal ageing on an unmodified short-term aged binder. A total of four different lamps (2 sunlight lamps with different power levels and two narrow band lamps at 365 and 405 nm) were used in the ageing experiments. The aged binders were analysed with FTIR spectroscopy, DSR and partially SARA fractionation. The results showed that pure photooxidation induced little to no ageing, while temperature alone leads to the well-known ageing effects. A surprising result was discovered when comparing the combined effect of light and temperature, where a synergistic effect caused a drastic increase in the ageing level. Furthermore, both sunlight lamps induced a similar level of ageing, while having a difference in intensity, which indicates that only a certain amount of photoenergy is needed to achieve this synergistic ageing effect. Comparison to multiple PAV aged binders shows that similar or higher ageing levels can be achieved when sun light is involved. This would be a great addition to an artificial ageing setup, as replacing the 'unrealistic' high pressure with a factor that occurs in the field will be beneficial to simulate ageing in a more realistic way.

The influence of different wavelength domains (same energy level) showed that while all lamps induced a similar formation of carbonyls and sulfoxides, their impact on the rheological level and SARA

fractions differs. The sunlight aged binder reached a higher rheological level, followed by the UV light aged binder and the blue light aged binder having the lowest stiffness values and overall polarity shift. This indicates not only that the wavelength domain matters for the ageing process but also that a possible synergistic effect between different wavelengths might accelerate the ageing process even more.

Overall these results shed light on how photooxidation and thermal ageing influence the ageing behaviour of bitumen, which highlights not only the necessity to consider artificial sun light within the visible domain in the laboratory ageing simulation but also understand which parts of the sun light spectrum contribute most to it.

Acknowledgements

The financial support by the Austrian Federal Ministry for Digital and Economic Affairs, the National Foundation for Research, Technology and Development and the Christian Doppler Research Association is gratefully acknowledged. Furthermore, the authors would also like to express their gratitude to the CD laboratories company partners BMI Group, OMV Downstream and Pittel+Brausewetter for their financial support. The authors acknowledge TU Wien Bibliothek for financial support through its Open Access Funding Programme.

Disclosure statement

No potential conflict of interest was reported by the author(s).

Funding

This work was supported by Christian Doppler Forschungsgesellschaft: [Grant Number 1836999].

ORCID

Johannes Mirwald  <http://orcid.org/0000-0001-5025-7427>

Kristina Primerano  <http://orcid.org/0000-0001-5978-1989>

Bernhard Hofko  <http://orcid.org/0000-0002-8329-8687>

References

- Adolfo, F. R., Claussen, L. E., Cargnin, R. S., Brudi, L. C., Grasmann, C. S., Nascimento, P. C. D., Cravo, M., Nascimento, L. A., Alcantara, A. P. M. P., Branco, V. T. F. C., & de Carvalho, L. M. (2022). Influence of thermal aging and long term-aging on Ni and V content in asphalt fractions and their determination in air particulate matter from asphalt mixing plants. *Fuel*, 324, 124289. <https://doi.org/10.1016/j.fuel.2022.124289>
- Atkinson, R. (2000). Atmospheric chemistry of VOCs and NOx. *Atmospheric Environment*, 34(12), 2063–2101. [https://doi.org/10.1016/S1352-2310\(99\)00460-4](https://doi.org/10.1016/S1352-2310(99)00460-4)
- Camargo, I., Hofko, B., Mirwald, J., & Grothe, H. (2020). Effect of thermal and oxidative aging on asphalt binders rheology and chemical composition. *Materials (Basel)*, 13(19), 4438. <https://doi.org/10.3390/ma13194438>
- CEN. (2012a). EN 14769: Bitumen and bituminous binders - Accelerated long-term ageing conditioning by a Pressure Ageing Vessel (PAV). In Brussels.
- CEN. (2012b). EN 14770: Bitumen and bituminous binders - Determination of complex shear modulus and phase angle - Dynamic Shear Rheometer (DSR). In Brussels.
- CEN. (2015). EN 12607-1: Bitumen and bituminous binders - Determination of the resistance to hardening under the influence of heat and air - Part 1: RTFOT method. In Brussels.
- de Sá Araujo, M. D. F. A., Lins, V. D. F. C., Pasa, V. M. D., & Leite, L. F. M. (2013). Weathering aging of modified asphalt binders. *Fuel Processing Technology*, 115, 19–25. <https://doi.org/10.1016/j.fuproc.2013.03.029>
- Feng, Z.-G., Bian, H.-J., Li, X.-J., & Yu, J.-Y. (2015). FTIR analysis of UV aging on bitumen and its fractions. *Materials and Structures*, 49(4), 1381–1389. <https://doi.org/10.1617/s11527-015-0583-9>
- Hofer, K., Mirwald, J., Maschauer, D., Grothe, H., & Hofko, B. (2022). Influence of selected reactive oxygen species on the long-term aging of bitumen. *Materials and Structures*, 55(5), 133. <https://doi.org/10.1617/s11527-022-01981-1>
- Hu, M., Ma, J., Sun, D., Hofko, B., Mirwald, J., Zheng, Y., & Xu, L. (2022). Quantifying weathering-aging test parameters of high viscosity-modified asphalt by establishing a conversion relationship with standard PAV aging. *Journal of Materials in Civil Engineering*, 34(6), 04022089. [https://doi.org/10.1061/\(ASCE\)MT.1943-5533.0004228](https://doi.org/10.1061/(ASCE)MT.1943-5533.0004228)
- Hung, A., & Fini, E. H. (2020). Surface morphology and chemical mapping of UV-aged thin films of bitumen. *Acs Sustainable Chemistry & Engineering*, 8(31), 11764–11771. <https://doi.org/10.1021/acssuschemeng.0c03877>

- Hung, A. M., Goodwin, A., & Fini, E. H. (2017). Effects of water exposure on bitumen surface microstructure. *Construction and Building Materials*, 135, 682–688. <https://doi.org/10.1016/j.conbuildmat.2017.01.002>
- Hung, A. M., Kazembeyki, M., Hoover, C. G., & Fini, E. H. (2019). Evolution of morphological and nanomechanical properties of bitumen thin films as a result of compositional changes due to ultraviolet radiation. *ACS Sustainable Chemistry & Engineering*, 7(21), 18005–18014. <https://doi.org/10.1021/acssuschemeng.9b04846>
- Larkin, P. (2011). *Infrared and Raman spectroscopy*. Elsevier.
- Li, Y., Wu, S., Liu, Q., Dai, Y., Li, C., Li, H., Nie, S., & Song, W. (2019). Aging degradation of asphalt binder by narrow-band UV radiations with a range of dominant wavelengths. *Construction and Building Materials*, 220, 637–650. <https://doi.org/10.1016/j.conbuildmat.2019.06.035>
- Ma, L., Varveri, A., Jing, R., & Erkens, S. (2021). Comprehensive review on the transport and reaction of oxygen and moisture towards coupled oxidative ageing and moisture damage of bitumen. *Construction and Building Materials*, 283, 122632. <https://doi.org/10.1016/j.conbuildmat.2021.122632>
- Maschauer, D., Mirwald, J., Hofko, B., & Grothe, H. (2020). Viennese Aging Procedure (VAPro): Adaption for Low-temperature testing. In *Proceedings of the RILEM International Symposium on Bituminous Materials* (Vol. 27, pp. 1933–1939). Springer. https://doi.org/10.1007/978-3-030-46455-4_245
- Mirwald, J., Maschauer, D., Hofko, B., & Grothe, H. (2020). Impact of reactive oxygen species on bitumen aging – The viennese binder aging method. *Construction and Building Materials*, 257, 119495. <https://doi.org/10.1016/j.conbuildmat.2020.119495>
- Mirwald, J., Nura, D., Eberhardsteiner, L., & Hofko, B. (2022a). Impact of UV–Vis light on the oxidation of bitumen in correlation to solar spectral irradiance data. *Construction and Building Materials*, 316, 125816. <https://doi.org/10.1016/j.conbuildmat.2021.125816>
- Mirwald, J., Nura, D., & Hofko, B. (2022b). Recommendations for handling bitumen prior to FTIR spectroscopy. *Materials and Structures*, 55(2), 26. <https://doi.org/10.1617/s11527-022-01884-1>
- Petersen, J. C. (1984). Chemical composition of asphalt as related to asphalt durability: State of the Art. *Transp. Res. Rec*, 999, 13–30.
- Petersen, J. C. (2006). *Oxidative aging model WRI–FHWA Symposium, Models Used to Predict Pavement Performance*, Laramie, Wyo.
- Petersen, J. C. (2009). A review of the fundamentals of asphalt oxidation: Chemical, physicochemical, physical property, and durability relationships. In *TRB Transportation Research Circular E-C140*. Transportation Research Board of the National Academies. <https://doi.org/10.17226/23002>
- Petersen, J. C., Barbour, R. V., Dorrence, S. M., Barbour, F. A., & Helm, R. V. (2002). Molecular interactions of asphalt. Tentative identification of 2-quinolones in asphalt and their interaction with carboxylic acids present. *Analytical Chemistry*, 43(11), 1491–1496. <https://doi.org/10.1021/ac60305a012>
- Petersen, J. C., & Glaser, R. (2011). Asphalt oxidation mechanisms and the role of oxidation products on age hardening revisited. *Road Materials and Pavement Design*, 12(4), 795–819. <https://doi.org/10.1080/14680629.2011.9713895>
- Sakib, N., & Bhasin, A. (2018). Measuring polarity-based distributions (SARA) of bitumen using simplified chromatographic techniques. *International Journal of Pavement Engineering*, 20(12), 1371–1384. <https://doi.org/10.1080/10298436.2018.1428972>
- Sreeram, A., Masad, A., Sootodeh Nia, Z., Maschauer, D., Mirwald, J., Hofko, B., & Bhasin, A. (2021). Accelerated aging of loose asphalt mixtures using ozone and other reactive oxygen species. *Construction and Building Materials*, 307, 124975. <https://doi.org/10.1016/j.conbuildmat.2021.124975>
- Zeng, W. B., Wu, S. P., Pang, L., Chen, H. H., Hu, J. X., Sun, Y. H., & Chen, Z. W. (2018). Research on Ultra Violet (UV) aging depth of asphalts. *Construction and Building Materials*, 160, 620–627. <https://doi.org/10.1016/j.conbuildmat.2017.11.047>